The Design of Radar Signals Having Both High Range Resolution and High Velocity Resolution

By J. R. KLAUDER

(Manuscript received April 5, 1960)

Radar systems that yield simultaneous information regarding the range and velocity of a target would be useful in certain applications. A discussion is presented of some fundamental limitations on simultaneous range-velocity determination in terms of ambiguity diagrams, with the aid of a quantum mechanical analog to the Wigner distribution function. A sequence of signals is found in which the signals yield both range and velocity information with increasing accuracy. However, this desired property is not accompanied by a waveform suitable for maximum operating efficiency.

I. INTRODUCTION

The very large power requirements of present-day radars clearly demand full utilization of the potential of existing equipment. Unfortunately, an efficient equipment use does not always lead directly to a signal possessing desired high resolution characteristics. The "Chirp" scheme, which employs linear frequency modulation and is discussed in detail in the accompanying paper,[1] represents one method by which the desirable high resolution properties may be secured with an optimum equipment utilization. However, in Section 3.5 of the accompanying paper it was pointed out that the Chirp scheme, like ordinary radar techniques, possesses an inherent ambiguity in a simultaneous determination of both the range and velocity of a moving target. Ambiguity diagrams,[2] which are representations of joint response functions in both time and Doppler frequency, provide a pictorial representation of the uncertainty in determining range (time) and velocity (Doppler frequency). Fig. 1, (which is a duplicate of Fig. 38 of the accompanying paper) schematically illustrates the ambiguity diagrams corresponding to three different transmitted signals: (a) a long constant-frequency sig-

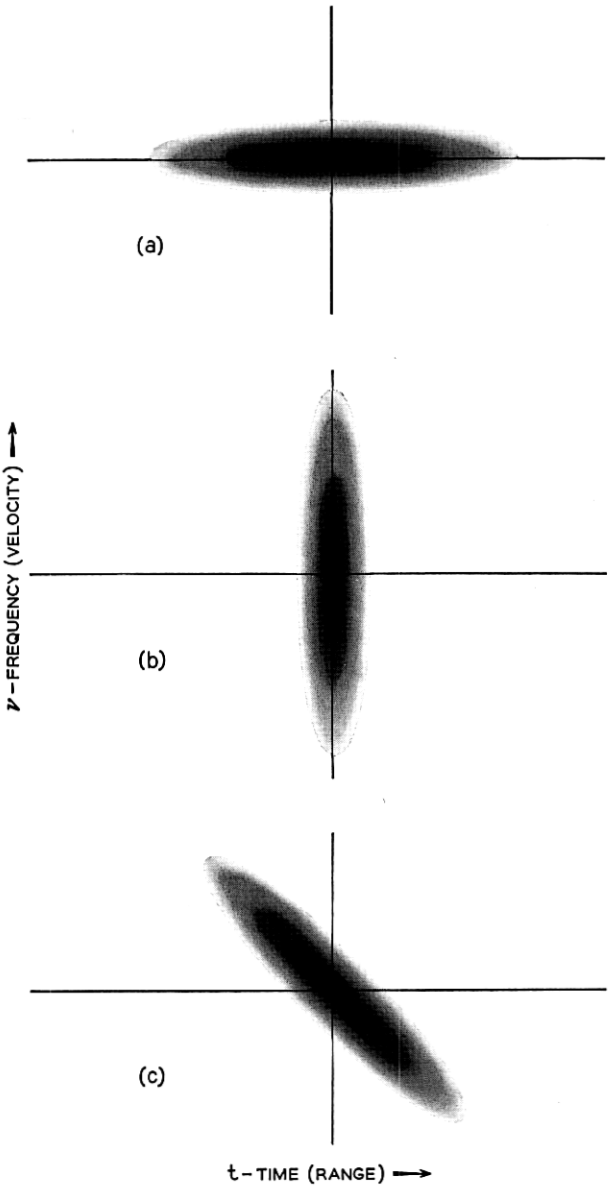

Fig. 1 — (a) Schematic ambiguity diagram for a long constant-frequency radar signal; the more shaded portions denote regions of greater signal response with time, t, and for variously moving targets with Doppler frequency, ν. (b) Schematic ambiguity diagram for a short constant-frequency radar signal; improved time resolution is secured at the expense of some discrimination against moving targets. (c) Schematic ambiguity diagram for a typical Chirp signal; an approaching target with a positive Doppler shift has a response attentuated in amplitude and shifted to an earlier time.

nal, (b) a very short constant-frequency signal and (c) a Chirp signal with linear frequency modulation.

For certain applications it may be desirable to transmit a signal whose ambiguity function is highly peaked only about the point $t = \nu = 0$. If such a signal exists, it would permit a high resolution in both range and velocity simultaneously. In Section II of this paper some properties of ambiguity functions are discussed with the aid of quantum mechanical analogs, and one interesting general property is discussed in detail: If a requirement of rotational invariance is imposed on ambiguity functions (a concept made precise in Section II) a sequence of signals is obtained for which the peaking of the ambiguity function is steadily increased. While the signals in this class achieve the desired behavior in the ambiguity function, the transmitter waveforms are not uniform in amplitude and, therefore, cannot be transmitted with the same efficiency as the uniform amplitude Chirp signal. The notation used in the following analysis is the same as that in the accompanying paper.

II. SOME GENERAL PROPERTIES OF AMBIGUITY DIAGRAMS

For convenience in the analysis, only a single target, which gives rise to a Doppler shift $\nu = vf_{RF}/c$ is studied, where v is the target velocity, f_{RF} is the radio-frequency carrier and c is the velocity of light. If the spectrum of an arbitrary complex transmitted signal is denoted by $\tilde{\epsilon}(f)$ then the received signal becomes $\tilde{\epsilon}(f - \nu)$. Only receiving networks that optimize the signal-to-noise ratio will be discussed. For an arbitrary complex signal $\epsilon(t)$, this optimum filter is the so-called matched filter for that signal. If $\tilde{\epsilon}(f)$ denotes the Fourier transform of the signal $\epsilon(t)$, then the matched filter $\tilde{Y}_m(f)$ may be defined[1] as $\tilde{\epsilon}^*(f)$. With a matched filter in the receiver, the response spectrum is determined by $\tilde{\epsilon}^*(f)\tilde{\epsilon}(f - \nu)$. The Fourier transform determines the time response:

$$\chi(t,\nu) = \int_{-\infty}^{\infty} \tilde{\epsilon}^*(f)\tilde{\epsilon}(f - \nu)e^{2\pi ift}\, df, \tag{1}$$

which is written as a two-parameter function. This is the expression given by Woodward,[2] and can be used perfectly well to specify the ambiguity diagrams. However, for the analogy to be drawn to single-particle nonrelativistic quantum mechanics, it is convenient to develop an alternate expression for the ambiguity function amplitude.

Suppose that the transmitter spectrum, $\tilde{\epsilon}(f)$, is concentrated about some high RF frequency, so that

$$\tilde{\epsilon}(f) = \tilde{\mathcal{E}}(f - f_{RF}), \tag{2a}$$

where $\tilde{\mathcal{E}}(f)$ is a spectrum centered about zero frequency. It follows from (2a) that

$$\epsilon(t) = \mathcal{E}(t)e^{2\pi i f_{RF} t}. \tag{2b}$$

Therefore, $\mathcal{E}(t)$ represents the generalized envelope of the transmitted signal. If (2a) is substituted into (1), one readily finds that

$$\chi(t,\nu) = e^{2\pi i (f_{RF}+\nu/2)t} \int_{-\infty}^{\infty} \tilde{\mathcal{E}}^* \left(f + \frac{\nu}{2}\right) \tilde{\mathcal{E}} \left(f - \frac{\nu}{2}\right) e^{2\pi i f t}\, df, \tag{3a}$$

or, when expressed in terms of $\mathcal{E}(t)$,

$$\chi(t,\nu) = e^{2\pi i (f_{RF}+\nu/2)t} \int_{-\infty}^{\infty} \mathcal{E}^* \left(\tau - \frac{t}{2}\right) \mathcal{E} \left(\tau + \frac{t}{2}\right) e^{2\pi i \nu \tau}\, d\tau. \tag{3b}$$

Let the carrier in the presence of a Doppler shift be taken as $f_{RF} + \nu/2$. With this choice of carrier,

$$\rho(t,\Omega) = \int_{-\infty}^{\infty} \mathcal{E}^* \left(\tau - \frac{t}{2}\right) \mathcal{E} \left(\tau + \frac{t}{2}\right) e^{i\Omega\tau}\, d\tau \tag{4}$$

is defined to be the complex two-parameter response envelope. For convenience, the Doppler angular frequency $\Omega = 2\pi\nu$ has been introduced in (4). It is the absolute value of $\rho(t,\Omega)$, which represents the detected output. The remaining analysis uses the definition made in (4); it is also the form studied by Gabor[3] and Ville.[4]

No loss of generality is made by assuming the transmitted signal carries unit energy:

$$\int_{-\infty}^{\infty} |\, \epsilon(t)\,|^2\, dt = \int_{-\infty}^{\infty} |\, \mathcal{E}(t)\,|^2\, dt = \int_{-\infty}^{\infty} |\, \tilde{\mathcal{E}}(f)\,|^2\, df = 1. \tag{5}$$

With this normalization, it follows from (4) that

$$\rho(0,0) = \int_{-\infty}^{\infty} |\, \mathcal{E}(\tau)\,|^2\, d\tau = 1. \tag{6}$$

This result represents a constraint that requires a portion of the "ambiguity" to remain in the vicinity of the point $t = \Omega = 0$. By a straightforward integration using (4) and (5), the following result may be established:

$$\frac{1}{2\pi} \int_{-\infty}^{\infty} \int_{-\infty}^{\infty} |\, \rho(t,\Omega)\,|^2\, dt\, d\Omega = 1. \tag{7}$$

[This result applies equally well to a similar integration involving $\chi(t,\nu)$.] The interpretation given to (7) is as follows: There is, quali-

tatively speaking, a total ambiguity equal to "one", which must be distributed throughout the t,Ω plane. The approximately equal amounts of shaded area in Fig. 1 are intended to be a reflection of this constraint. This result seems to preclude any simple solution to achieve simultaneously an arbitrarily high resolution in both range and velocity.

Another observation worth making about the three diagrams in Fig. 1 is that it appears they could be obtained from one another by a "rotation" about the origin of the t,Ω plane. It will be demonstrated below that this is a general result. That is, for every ambiguity diagram defined by $\rho(t,\Omega)$ there exists another signal that generates another diagram differing from the first only by a rotation about $t = \Omega = 0$. The use of the word "rotation" needs some explanation here. Actually, the rotation can proceed along arbitrary elliptical contours. However, for convenience, it is assumed that the scales of time and Doppler frequency have been chosen so that the rotation is nearly circular.

The rotation theorem, as well as others like it, is most readily established by using methods common in the study of quantum mechanics. One of the reasons for choosing the form of (4) in preference to that of (1) was to facilitate the comparison with a quantity studied previously in quantum mechanics. Only a brief sketch is presented here of the comparison used to obtain most of the remaining results of this section.

The quantity of interest in quantum mechanics is the so-called Wigner[5] distribution function defined by

$$P(q,p) = \frac{1}{h}\int_{-\infty}^{\infty} \psi^*\left(q - \frac{y}{2}\right) e^{-iyp/\hbar}\psi\left(q + \frac{y}{2}\right) dy. \tag{8}$$

Here, $h = 2\pi\hbar$ is Planck's constant and $\psi(y)$ represents the Schrödinger wave function for a single particle in one dimension. Of more direct interest is the characteristic function for this distribution, i.e. its double Fourier transformation:

$$\begin{aligned} \rho(y,\kappa) &= \int P(q,p)e^{i(\kappa q+yp)/\hbar}\, dq\, dp, \\ &= \int \psi^*\left(q - \frac{y}{2}\right)e^{i\kappa q/\hbar}\psi\left(q + \frac{y}{2}\right) dq. \end{aligned} \tag{9}$$

If this result is compared with (4), one notes an exact functional equivalence, with t playing the role of y and Ω playing the role of $\kappa/\hbar$. Equation (9) is perhaps easier than (8) to study, and has been treated in some detail by Bass,[6] Moyal[7] and Groenewold;[8] further references may be found in these works. The relative simplicity of (9) stems from its simple representation in the quantum mechanical Hilbert space:

$$\rho(y,\kappa) = (\Psi, e^{i(\kappa\mathbf{q}+\nu\mathbf{p})/\hbar}\Psi). \tag{10}$$

Here Ψ denotes an arbitrary normalized vector and $\mathbf{q}$ and $\mathbf{p}$ are the usual operators satisfying $\mathbf{qp} - \mathbf{pq} = i\hbar$. Numerous additional relations may be found, especially in the work of Moyal.

The necessary signal transformation to generate a rotated ambiguity diagram will not be derived; the result will be stated without proof. Suppose that $\mathcal{E}(t)$ is an envelope which generates a particular ambiguity function $\rho(t,\Omega)$ according to (4). The modified envelope, $\mathcal{E}_\theta(t)$, must be chosen so that its ambiguity function is defined by

$$\rho_\theta(t,\nu) = \rho\left(t\cos\theta + \frac{\nu}{\gamma}\sin\theta,\ \nu\cos\theta - \gamma t\sin\theta\right). \tag{11}$$

Here, γ represents the ratio of the "angular frequency" axis to the "time" axis of the ellipse of rotation and θ represents the "angle" of rotation. When $\gamma \approx 1$, rotation is along nearly circular orbits. The solution for $\mathcal{E}_\theta(t)$ is given by

$$\mathcal{E}_\theta(t) = \int_{-\infty}^{\infty} U(t,\tau;\theta)\mathcal{E}(\tau)\,d\tau, \tag{12}$$

where the kernel $U(t,\tau;\theta)$ is expressed as follows:

$$U(t,\tau;\theta) = \sqrt{\frac{\gamma}{2\pi i\sin\theta}}\exp\left\{i\gamma\left[\left(\frac{t^2+\tau^2}{2}\right)\cot\theta - t\tau\csc\theta\right]\right\}. \tag{13}$$

Equation (13) follows from the properties of the well-known harmonic oscillator problem, and is just one of the relations readily obtained with the techniques of quantum mechanics.

The particular relations expressed in (12) and (13) are perhaps not as interesting as an additional result that can be derived from them. In the discussion of the ambiguities present in the interpretation of the diagrams in Fig. 1 it seemed that the resolution was relatively good in one direction but was poor in the perpendicular direction. It is just such a variation with direction that is *not* wanted in attempting to achieve a signal whose ambiguity function is concentrated about the point $t = \Omega = 0$. For clarity, assume again that the t and Ω axes have already been scaled for the specific system under study. Then, to secure (as nearly as possible) an ambiguity diagram concentrated about the origin, it appears desirable to seek a *rotational invariance of the ambiguity function*; i.e., $\rho_\theta(t,\Omega) = \rho(t,\Omega)$. It is a simple matter to demonstrate that $\rho_\theta(t,\Omega) = \rho(t,\Omega)$ if and only if

$$\mathcal{E}_\theta(t) = \int_{-\infty}^{\infty} U(t,\tau;\theta)\mathcal{E}(\tau)\,d\tau = e^{-i\lambda\theta}\mathcal{E}(t), \tag{14}$$

where λ represents a suitable constant. There are a denumerable number of solutions to (14), a typical one being denoted by $\mathcal{E}_n(t)$, where $\lambda_n = n + \frac{1}{2}$. These solutions, familiar as the eigenfunctions of the harmonic oscillator, are defined by the following relation:

$$\mathcal{E}_n(t) = \frac{\gamma^{\frac{1}{4}}}{\sqrt{\pi^{\frac{1}{2}} n! 2^n}} H_n(\sqrt{\gamma} t) e^{-\gamma t^2/2}, \tag{15}$$

where $H_n(z)$ represents the nth Hermite polynomial defined, for example, by

$$\mathrm{H}_n(z) = (-1)^n e^{z^2} \frac{d^n}{dz^n} e^{-z^2}. \tag{16}$$

Figs. 2(a), 3(a), 4(a) and 5(a) show four curves of $\mathcal{E}_n(t)$ for $n = 0$, 4, 10 and 26, respectively; each curve is symmetric about $t = 0$ and is only shown for positive values of t. Note also a change in scale in the different figures. In each example γ was chosen equal to one.

It is a well-known fact that the functions $\mathcal{E}_n(t)$ defined by (15) have spectra, $\tilde{\mathcal{E}}_n(f)$, which are specified by the very same functional form.† Consequently, Figs. 2(a) through 5(a) also represent the frequency spectra for the same n values. One can see from these four figures that, as n increases, both the pulse width and bandwidth increase. The pulse-width-bandwidth product increases as $(n + \frac{1}{2})^2$ as n is increased. One may hope, therefore, that the ambiguity function becomes more nearly concentrated about the origin as n increases. The normalization condition (7) must still be satisfied, but, for large n, the remaining "ambiguity" is thinly spread out over a large region of the t,Ω plane.

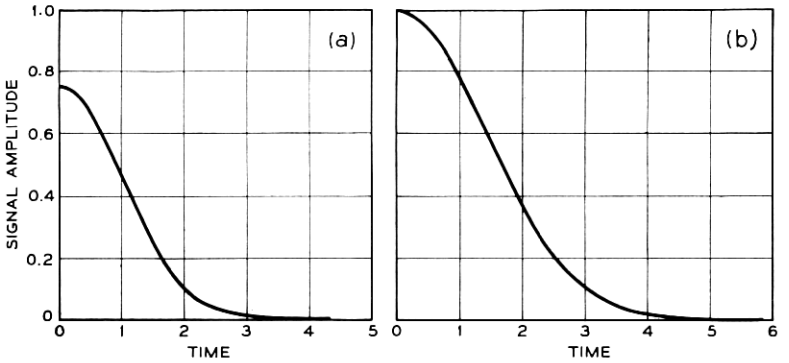

Fig. 2 — (a) Envelope of the transmitted signal when the parameter $n = 0$; in this case the curve is gaussian. (b) Envelope of the "rotationally invariant" matched-filter response when $n = 0$; here the curve is also gaussian.

† See Pair 702 in the tables of Campbell and Foster.[9]

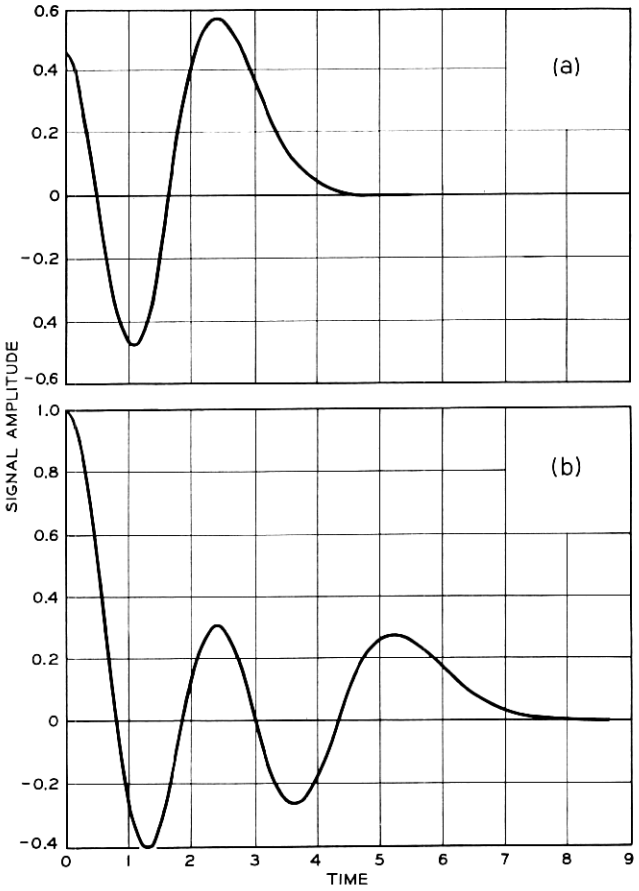

Fig. 3 — Envelope of (a) transmitted signal and (b) matched-filter response when $n = 4$.

This interpretation may be verified in detail by evaluating the ambiguity function $\rho_n(t,\Omega)$ when $\mathcal{E}(t)$ is given by $\mathcal{E}_n(t)$. In this calculation it is advantageous to employ the result that $\rho_n(t,\Omega)$ will, by construction, be rotationally symmetric. Hence, it suffices to study the cross section of the ambiguity diagram when $\Omega = 0$; the complete contour may be reconstructed by rotation about the point $t = \Omega = 0$. It is an interesting fact that the kernel $U(t,\tau;\theta)$ can be rapidly converted into a generating function for the various response signals $\rho_n(t,0)$. The details of such a calculation are essentially present in the work of Moyal.[7] Either from the generating function or by a direct use of the definition for $\rho(t,\Omega)$ one finds the zero Doppler response to be

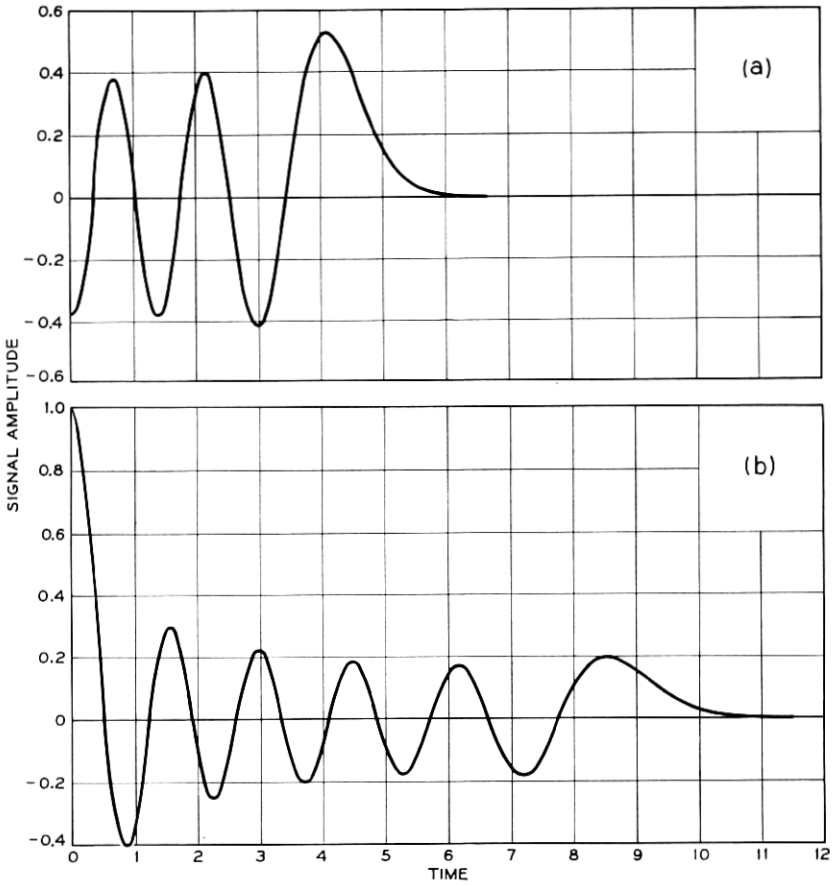

Fig. 4 — Envelope of (a) transmitted signal and (b) matched-filter response when $n = 10$.

$$\rho_n(t,0) = \frac{1}{n!} L_n\left(\frac{\gamma t^2}{2}\right) e^{-\gamma t^2/4}, \tag{17}$$

where $L_n(z)$ represents the nth Laguerre polynomial defined by

$$L_n(z) = e^z \frac{d^n}{dz^n}(z^n e^{-z}). \tag{18}$$

The output signal $\rho_n(t,0)$ is illustrated in Figs. 2(b), 3(b), 4(b) and 5(b) for $n = 0$, 4, 10 and 26, respectively. Since these functions are clearly symmetric only positive t values have been included (note the change

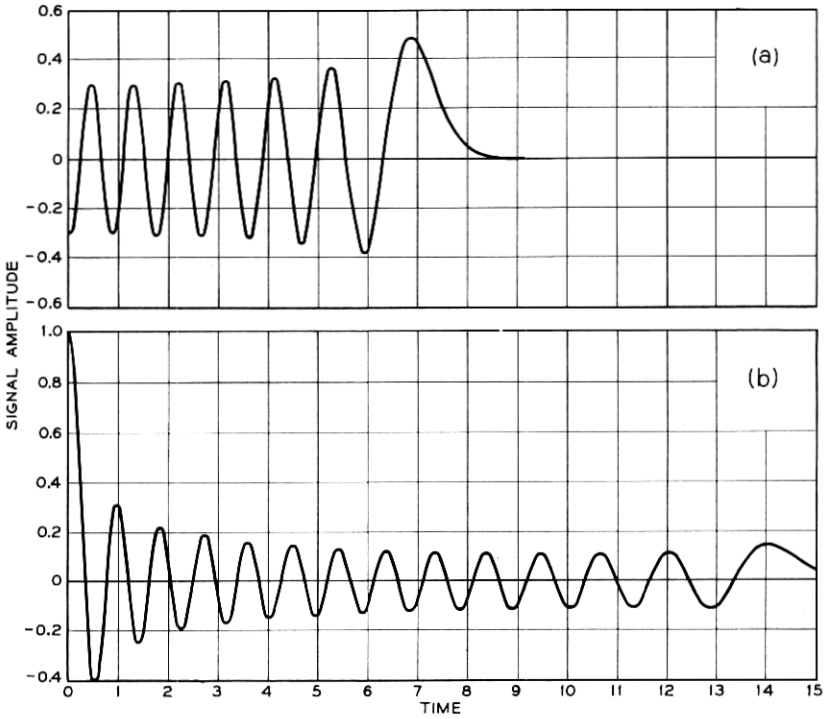

Fig. 5 — Envelope of (a) transmitted signal and (b) matched-filter response when $n = 26$.

of scale in the different figures). Again, these curves were obtained assuming $\gamma = 1$. In order to illustrate the rotationally invariant character of these signals, Fig. 6 shows a cut-away of a three-dimensional projected view of the complete ambiguity amplitude $\rho(t,\Omega)$ corresponding to the case $n = 10$.

Fig. 6 illustrates the tendency of the ambiguity function to peak about the origin of the t,Ω plane. Furthermore, it demonstrates that a narrow peak is achieved only when the remaining "ambiguity" is spread out over a relatively large domain of the t,Ω plane.

If input and response envelopes ($\mathcal{E}_n(t)$ and $\rho_n(t,\Omega)$) with higher values of n are considered, the ambiguity function becomes more sharply peaked and more spread out. A study of the behavior of the zero Doppler response for large values of n shows that

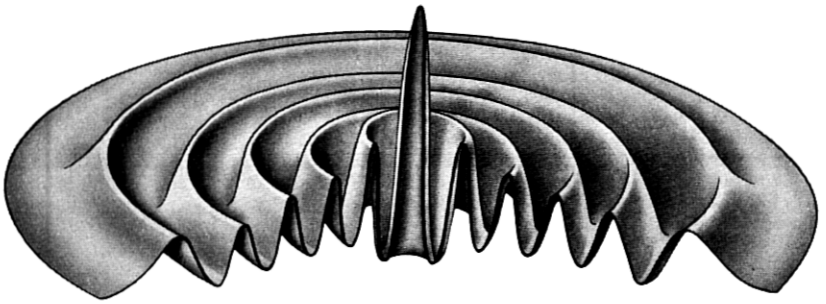

Fig. 6 — Cut-away of three-dimensional projected view of complete ambiguity amplitude $\rho(t,\Omega)$ when $n = 10$.

$$\rho_n(t,0) \sim J_0(\sqrt{2\gamma n}\, t), \tag{19}$$

where J_0 is the zeroth-order Bessel function. This asymptotic form is valid when t is greater than $\sqrt{n}$ but not so large that t becomes comparable with n itself. Equation (19) illustrates that, as n increases, the *form* of the response does not markedly change, only the *scale* changes. While the "rotationally invariant" response signals discussed here possess a narrow 3-db pulse width, they are endowed with long oscillatory tails, which fall off approximately as $t^{-\frac{1}{2}}$. This rate of fall-off is to be compared with the rate of fall-off of the Chirp signal — namely, as t^{-1}, which follows from (19) of the accompanying paper. Therefore, in securing an ambiguity function highly peaked about the origin a penalty must be paid in the rate of fall-off of the time "side lobes." Nevertheless, as the parameter n increases there is a change of scale and the side lobes are pulled inward. Consequently, at least in principle, a signal $\mathcal{E}_n(t)$ could be chosen that maintained side-lobe levels below an arbitrary level outside a prescribed ellipse in the t,Ω plane. It is interesting to speculate whether there exists some signal envelope $\mathcal{E}(t)$ that could be efficiently transmitted in addition to having a highly peaked ambiguity function. Unfortunately, this question remains unanswered.

III. ACKNOWLEDGMENTS

It is a pleasure to thank Miss B. Cetlin for her assistance in the computations required in this work.

REFERENCES

1. Klauder, J. R., Price, A. C., Darlington, S. and Albersheim, W. J., this issue, p. 745.

2. Woodward, P. M., *Probability and Information Theory, with Applications to Radar*, McGraw-Hill, New York, 1953.
3. Gabor, D., J.I.E.E., **93,** Pt. III, 1946, p. 429.
4. Ville, J., Cables & Trans., **2,** 1948, p. 61.
5. Wigner, E., Phys. Rev., **40,** 1932, p. 749.
6. Bass, J., Compt. rend., **221,** 1945, p. 46.
7. Moyal, J. E., Proc. Camb. Phil. Soc., **45,** 1949, p. 99.
8. Groenewold, H. J., Physica, **12,** 1946, p. 405.
9. Campbell, G. A. and Foster, R. M., *Fourier Integrals for Practical Applications*, D. Van Nostrand Co., New York, 1942.